Journal of Electrostatics, 20 (1987) 43-57
Elsevier Science Publishers B.V., Amsterdam – Printed in The Netherlands

ELECTRON BEAM EXPERIMENTS AT HIGH ALTITUDES

R. C. Olsen

Physics Department, The University of Alabama in Huntsville, Huntsville, AL 35899 (U.S.A)

(Received August 18, 1986; accepted in revised form February 9, 1987)

SUMMARY

Experiments with the electron gun on the SCATHA satellite produced evidence of beam-plasma interactions, and heating of the low energy electrons around the satellite. These experiments were conducted near geosynchronous orbit, in the dusk bulge, and plasma sheet, with one short operation in the lobe regions, providing a range of ambient plasma densities. The electron gun was operated at 50 eV, with beam currents of 1, 10 and 100 μA. Also, a filament emitter was used in a mode where it was biased -100 V with respect to the satellite, at a current setting of 20 iA. Data from electrostatic analyzers and the DC electric field experiment show that the satellite charged to near the beam energy in sunlight, at sufficiently high beam currents. The electrostatic analyzers showed distribution functions which had peaks, or plateaus at energies greater than the satellite potential. These measurements indicate heating of the ambient plasma, at several Debye lengths from the satellite (several 10's of meters), with the heated plasma then accelerated into the satellite. It is likely that at times the 'ambient' cold plasma is in fact the photoelectron sheath generated by the satellite.

1. I. INTRODUCTION

a. Electron beam experiments

Electron beam experiments have been conducted in the ionosphere and magnetosphere for almost two decades, in order to investigate basic plasma processes, vehicle charging, and magnetospheric fields and structures. The field has been reviewed extensively and a comprehensive bibliography is not attempted here [1]. One element of such experiments which is of current interest is the occurrence of beam-plasma interactions. Most recently, such interest has been stirred by experiments with the Spacelab I SEPAC payload, both in flight and in ground tests. It has been suggested that a beam-plasma discharge is established in the region of the cargo bay [2]. An alternative suggestion is that space-charge oscillations in the beam cause the beam scattering [3]. In this work, data are considered from a high altitude satellite which also indicate interactions between an emitted electron beam and the ambient plasma.

Journal of Electrostatics, 20 (1987) 43-57
Elsevier Science Publishers B.V., Amsterdam – Printed in The Netherlands

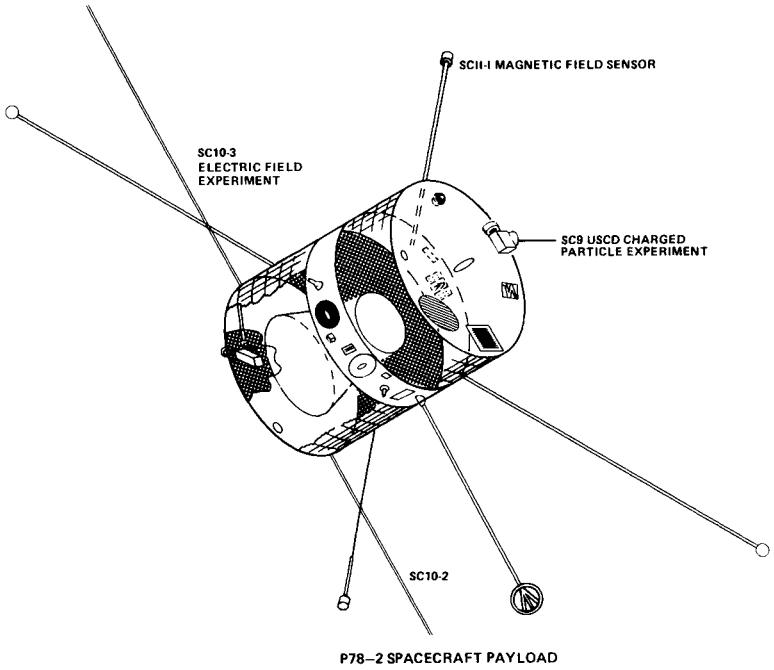

Figure 1. The SCATHA satellite.

b. Satellite and instruments

The P78-2 satellite was launched as part of the joint Air Force/NASA program to study Spacecraft Charging at High Altitudes and, is also called SCATHA [4]. SCATHA was launched on January 30, 1979 into a nearly geosynchronous orbit, with orbital parameters:

period	23h 5m
perigee	5.3 R_E
apogee	7.8 R_E
inclination	7.9°

The spin axis was nominally perpendicular to the earth-sun line, in the orbit plane, and the spin period was 59s. The cylindrically shaped satellite is shown in Figure 1. The 1.7 meter diameter, 1.75 meter high, satellite has a mixture of insulating and conducting surfaces. The 'top' of the satellite is a conducting surface, while the sides are primarily solar cell glass covers (insulators). There is a conducting belly band, and the 'bottom' is composed of insulators, particularly the injection motor cavity.

The electron gun experiment (designated SC4-1) was designed to conduct studies of induced satellite charging and discharging. Its primary purpose was to counter the large negative potentials routinely encountered in the midnight to dawn sector by geosynchronous satellites, such as ATS-6 and the kilovolt potentials measured in eclipse [5,6]

The electron gun could be operated at currents from 1ua to 1 mA, at beam voltages of 50 eV to 3 keV. It was not generally operated in the higher energy ranges, since major changes in satellite potential could he effected even at low currents. As shown in Figure 1, it is on the belly band, and the beam is directed radially away from the satellite. Data from SC4-1 experiments have been reported previously. [7,8]

In addition to the electron gun, there was a filament neutralizer associated with the ion accelerator (SC4-2) which could be operated independently. This package was located on the 'bottom' of the satellite. The neutralizer mode encountered in this article used a 100 V bias on the filament, and a current setting of 20 μA.

The UCSD particle detectors (SC-9) were mounted on the top of the satellite, on the side opposite the

Journal of Electrostatics, 20 (1987) 43-57
Elsevier Science Publishers B.V., Amsterdam – Printed in The Netherlands

electron gun. The detector consists of 5 electrostatic analyzers (ESA's). Two sets of paired ion and electron ESA's are mounted in rotating detector assemblies. The HI detectors cover the 1-eV to 81-keV energy range in 64 steps, while the LO detectors cover the 1-eV to 1800-eV energy range. The fifth ESA is fixed to the motor box, and covers the lower (1- to 1800-eV) energy range, for ions. The rotating detectors may rotate over a 220° range, including parallel to the spin axis, and radially away from the satellite. An energy sweep requires 16 seconds, and the detectors can be set to dwell on one energy step for up to 120 seconds. For practical purposes, pitch angle distributions are obtained by parking the detectors such that they point perpendicular to the spin axis, and high time resolution (of the 90° pitch angle particles) is obtained by parking a detector looking parallel to the spin axis. These detectors are similar to those flown on ATS-6.[9]

The GSFC electric field experiment (SC-10) consists of 2 cylindrical floating probes, 100m tip-to-tip. The probes are constructed of beryllium-copper tubing (.63 diameter), and are insulated for the first 30m (with a kapton coating), leaving 20m exposed conductor on each end. For purposes of measuring electric fields, the differential voltage (probe-to-probe) is measured. For our purposes, a more useful measurement is the 'common mode' voltage, the probe-to-satellite potential difference. Normally, this potential difference is small, varying by a few volts with spin due to probe illumination variations and a 1V spin modulation of the satellite potential caused by variations in the exposed conducting area [10,11]. During operations of the electron gun, however, the probe represents a reference point tied to the ambient plasma, and hence gives a measure of the change in the satellite potential. Unfortunately, the floating potential of the probe is perturbed by the gun operation, as shown in the data below, so the reference point is not as clear as initially hoped.[12]

2. OBSERVATIONS

Data from a sequence of operations on July 20, 1979 (Day 201) are presented first. Data from 0400 and 0600 UT are shown first illustrating experiments in the plasma sheet, near local midnight. The third example is from 2300 UT, near local dusk, in a region of higher density plasma. This is a disturbed day; ΣKp = 24+, Kp = 2+ for 3-6 UT, Kp = 4 for 21-24 UT. Following these data, data from April 1, 1979 (Day 91) are shown, in order to demonstrate the results of an eclipse of the satellite on an electron emission experiment.

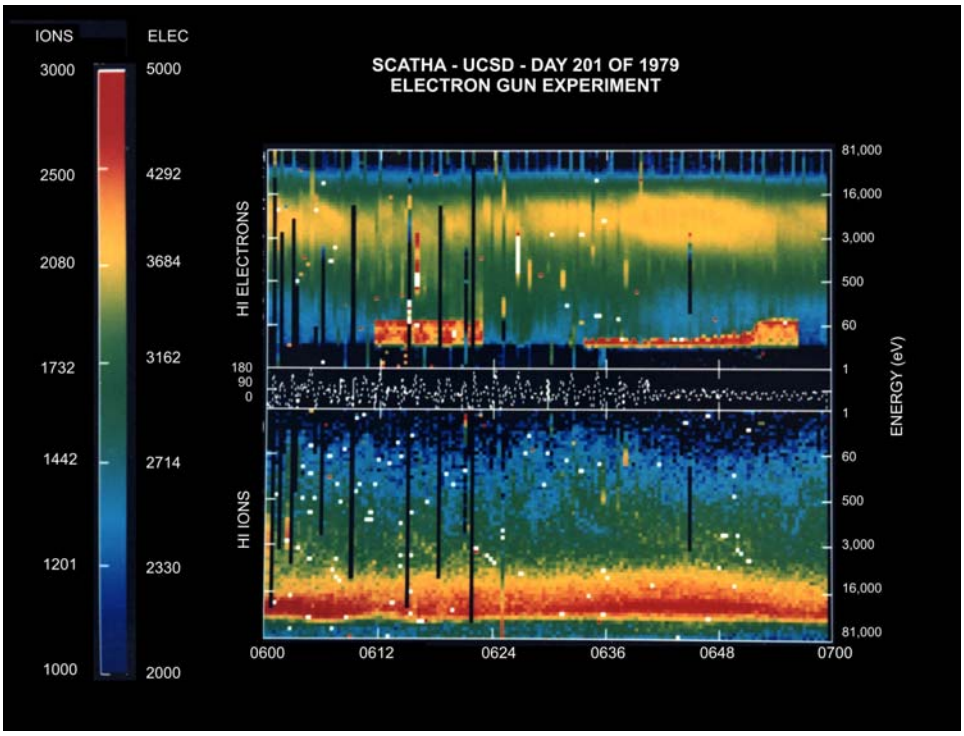

Figure 2. Energy time spectrogram for the UCSD high energy detectors.

Journal of Electrostatics, 20 (1987) 43-57
Elsevier Science Publishers B.V., Amsterdam – Printed in The Netherlands

A. 50 eV - 10uA - 0600 UT

The first example comes shortly after 0600 UT, at 0130 LT. The satellite is in the plasma sheet at 7.4 R_E, 17°λ_m, L = 8.8, and a dipole magnetic latitude of 23°. The plasma sheet electrons can be characterized with a density of 0.7 cm^{-3}, and temperature of 8.6 keV.

The data from this first operation are summarized in spectrogram format in Figure 2. In a spectrogram, the instrument count rate (or particle flux) is plotted as a function of time (horizontal axis) and energy (vertical axis), with high fluxes encoded with light gray or white, and low or zero fluxes encoded as black. Data from the two high energy detectors are shown here, with the electron data on top. The energy axis starts at zero in the middle of the figure, and in-creases upwards for electrons, and downwards for ions. The horizontal line plot along the center is the pitch angle of the measured particles, which is generally near 90° at this time. Two electron gun operation periods occur during this one hour time segment (0600-0700 UT). During the first segment, the gun is turned on, and high electron fluxes are found up to 70-80 eV for the entire period. In fact, the peak count rate, or flux, occurs in the 70-80 eV range, and not at 50 eV, as might be expected for a satellite charged to + 50 V. During the second operation visible in the figure, the satellite apparently did not initially charge to the gun energy, and high fluxes of electrons are found only up to a few tens of eV. There is then a subtle change in the keV electron and ion fluxes (a decrease) and the satellite potential apparently rises to near 50 V, and intense electron fluxes are found up to 70-80 eV. Data from the first operation are discussed next.

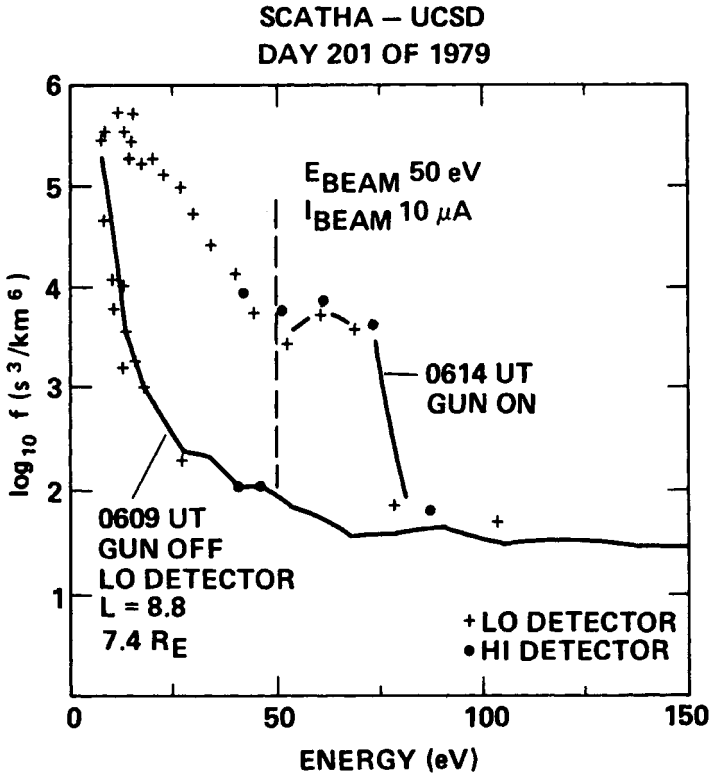

Figure 3. Electron distribution functions at 90° pitch angle, from the LO and HI detectors. Satellite is at 7.4 RE geocentric, L = 8.8, magnetic latitude 17°, 0125 MLT.

The 0-150 eV electron data are shown as a distribution function in Figure 3. In this format Maxwellian (e.g., thermalized) distributions will appear as straight lines. When the gun is off (0609 UT), the boundary between spacecraft generated photo electrons and ambient plasma at 10 to 15 eV suggests a satellite potential of +10 to +15 V [13,14]. When the gun is switched on, a different equilibrium is quickly

Journal of Electrostatics, 20 (1987) 43-57
Elsevier Science Publishers B.V., Amsterdam – Printed in The Netherlands

established. SCATHA charges to near the beam energy (50 eV), and enhanced fluxes appear both above and below 50 eV. There is not, however, a peak at 50 eV, as would be expected if the mono-energetic beam electrons returned to the satellite; nor is there a peak which could be attributed to cool (T ~ 1 eV) ambient electrons which have fallen through a 50 eV potential drop. Instead, there is a local minimum at 52 eV, and a peak above 50 eV, or at least a plateau from 55 to 75 eV. If the 0609 (gun off) data are shifted upwards in energy by 35 eV and if the only changes in the plasma measurements are those due to the increase in satellite potential, Liouville's theorem requires that the distribution functions overlap. They do so above about 80 eV, for the unperturbed magnetospheric plasma. It is clear from this comparison, however, that the 55 to 75 eV data represent a 'new' population, and do not simply represent a charging effect. The density in the 55 to 75 eV portion of the distribution function is about 1 cm^{-3}. This is comparable to the ambient density. The 20-45 eV electron data show a density of 124 cm^{-3}, and temperature of 6.3 eV.

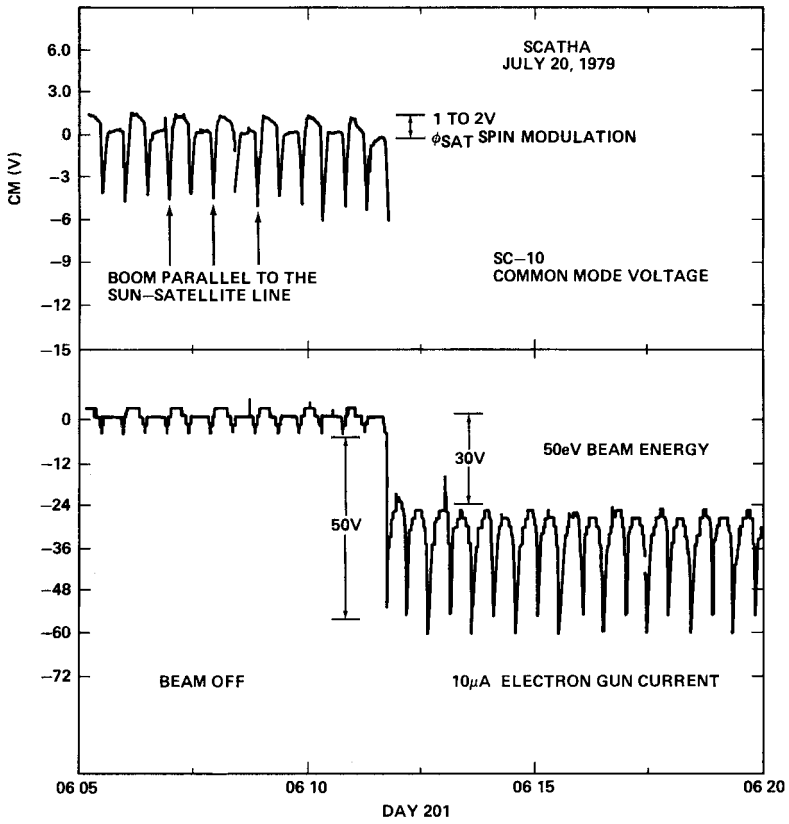

Figure 4 Common mode voltages at two ranges. The top section is from the ± 15 V channel, the bottom section from the ± 300 V channel.

The data from the electric field experiment are shown in Figure 4. The potential of the antenna with respect to the satellite drop by 30 to 50 V, depending on the spin phase. These data are consistent with a rise in satellite potential from about 15V to about +50V. The floating potentials of the antenna also rise, particularly during the portion of the spin when the antenna are perpendicular to the sun-satellite line. When the antenna are pointed along the sun-satellite line, they are at their most negative (with respect to the satellite), and it is inferred that the rise in antenna potential is at a minimum. The antenna potential are closest to plasma potential at this spin phase, both in sunlight and eclipse. The changes in antenna potential caused by the electron gun are attributed to an increase in the portion of emitted photoelectrons which escape from the antenna. The electrons emitted from the antenna are attracted to the highly positive satellite, instead of being reabsorbed by the antenna. The more positive satellite represents a sink for electrons emitted from the antenna [11,12]. These data therefore support the potentials inferred from the particle data, though there are ambiguities to these interpretations.

Journal of Electrostatics, 20 (1987) 43-57
Elsevier Science Publishers B.V., Amsterdam – Printed in The Netherlands

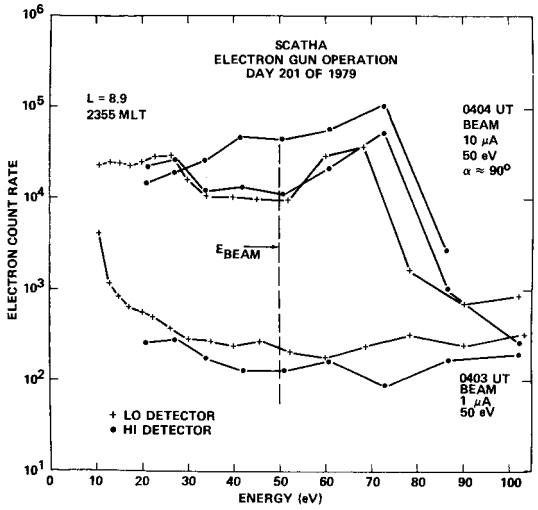

Figure 5. Electron count rate for electron gun currents of 1 μA and 10 μA. Satellite is at 7.7 RE geocentric, L = 8.9, magnetic latitude 14°, 2355 MLT.

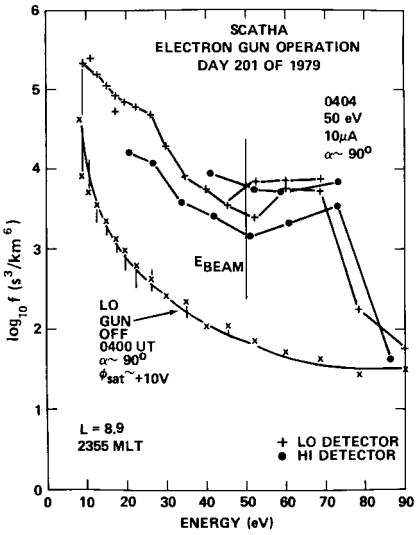

Figure 6. Electron distribution functions for zero beam current, and 10 μA beam current.

b. 50 eV - 10μA - 0400 UT

A second illustration of the observations resulting from 10pA beam current are given to emphasize the nature of the peak in flux, and occasionally even the distribution function. Figure 5 shows the count rate at beam currents of 1pA (0403 UT) and 10pA (0404. UT). The satellite does not respond measurably to the 1pA operation, and this is provided in lieu of "gun off" data as the baseline. The peak in count rate comes between 70 and 80 eV, as mentioned above. These data bear a striking resemblance to data taken during experiments with the SEPAC experiment on the shuttle SPACELAB-1 mission [3]. Figure 6 shows these data converted to distribution functions, and it is seen that event the distribution function exhibits a peak during some of the energy scans. Note that the adjacent energy points are taken at ¼ second intervals, the LO detector samples the 70 eV range 8 seconds after the HI detector, and the energy scans are 20 seconds apart. The differences in the four series of points shown here are attributed to rapid fluctuations in the environment, which are also apparent in the higher energy data. It seems reasonable to attribute the peaks near 70 eV to a consistent feature of the beam effects, since the peak is repeatable from scan to scan. Temporal fluctuation due to environmental variations cannot be completely ruled out, however, even over the one-second period required to scan the 50-80 eV energy range.

Data like these are found for several of the operational periods for this day and the following day. It was observed at an early stage of these experiments that there was a peak in the count rate (flux) at 70 eV during the 10 μA operations (shown here as a plateau in phase space density). A number of modifications of the UCSD detector's mode were made to focus on the phenomena, including dwelling at fixed energy levels from 50 to 70 eV for periods of up to 60 s. These data allowed comprehensive pitch angle coverage and provided a chance to determine if there were any obvious pitch angle effects. The answer was that none were found. The return peak showed no fluctuations during such dwells.

Journal of Electrostatics, 20 (1987) 43-57
Elsevier Science Publishers B.V., Amsterdam – Printed in The Netherlands

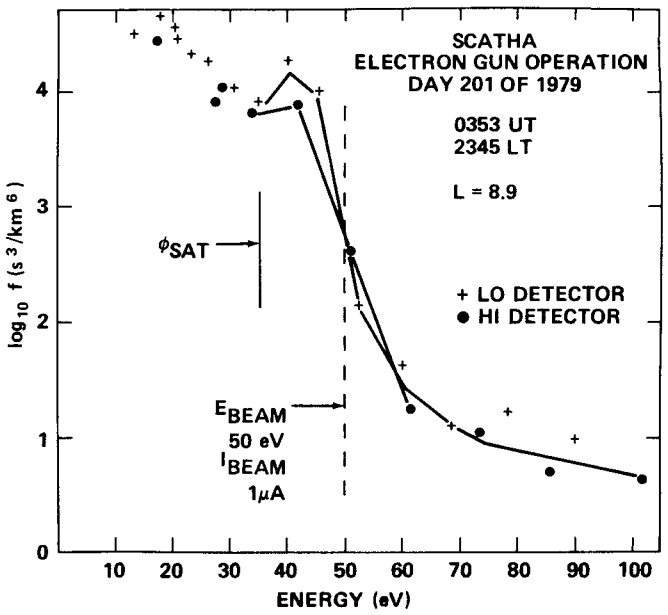

Figure 7. Electron distribution functions for 1 μA beam current in the tail lobe. Satellite is at 7.7 RE, L = 8.9, magnetic latitude 14°, 2345 MLT.

c. 50 eV - 1μA - 0353 UT

A few minutes prior to the above example, the satellite was in the tail lobe, as indicated by an apparent absence of plasma in the 1 eV to 80 keV energy range (ions and electrons). At such times, the ambient plasma density is of the order .01 cm^{-3}, in contrast to the 1.0 cm^{-3} plasma sheet environment encountered during the later experiments. Whereas the previous example indicated little or no effect due to a 1μA beam operation, a substantial effect is found in the third example. Figure 7 shows the electron distribution function for the 1μA operation at 0353. These spectra are interpreted as the result of a satellite potential of about +30V. Again, there is a peak in the distribution function just above the satellite potential, but at an energy *below* the beam energy.

Journal of Electrostatics, 20 (1987) 43-57
Elsevier Science Publishers B.V., Amsterdam – Printed in The Netherlands

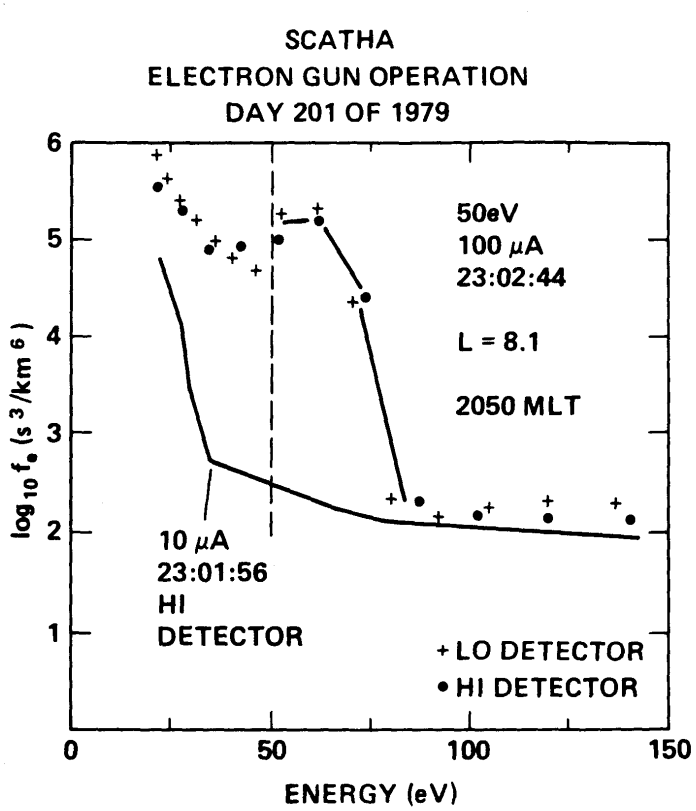

Figure 8. Electron distribution functions for 10 and 100 μA experiments in the dusk bulge. The satellite is at 7.5 R_E, L = 8.1, magnetic latitude 6°, 2050 MLT.

d. 50 eV - 100μA - 2300 UT

The fourth example comes from the dusk bulge, a region of higher ambient plasma density than the previous examples (1 to 10 cm^{-3}). Figure 8 shows the electron distribution functions for the beam at 10μA current, and 100μA current. The 10 μA operations results in an increase in the satellite potential to about +30V, but no peak above that energy. When the beam current is increased to 100 μA, the satellite potential increases to +50V, and a peak appears above 50 eV. This last pair of data sets indicate a trend of dependence of the satellite potential on ambient plasma density and beam current, which is expected. Also, there is a dependence of the 'plateau' effect on the ambient plasma conditions, and beam current. Unfortunately, it is difficulty to accurately determine the density of the low-energy background plasma at this time.

Journal of Electrostatics, 20 (1987) 43-57
Elsevier Science Publishers B.V., Amsterdam – Printed in The Netherlands

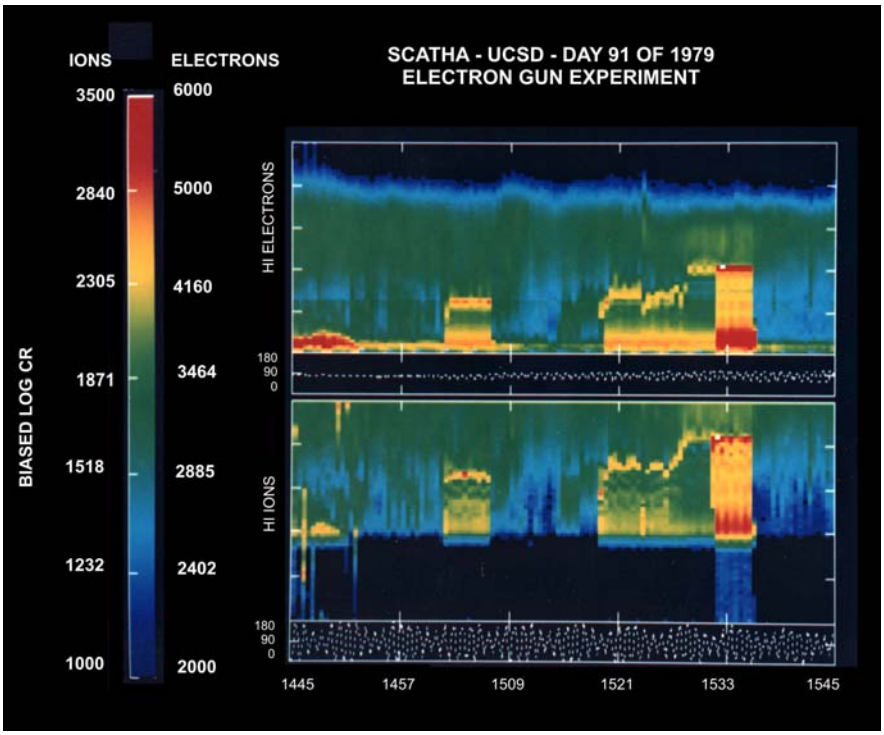

Figure 9. Energy-time spectrograms for the two UCSD electron detectors.

e. 100 eV - 20 μA - Eclipse

One possibility for the enhanced flux of (apparently) heated electrons is that these are heated photoelectrons. To shed some light on this idea, data taken in eclipse were sought for comparison. The data which are closest in nature to those shown above are for an experiment with the filament electron emitter associated with the ion gun. On April 1, 1979 (Day 91), the satellite was in eclipse, and charged to near zero volts when the filament was turned on. The filament was biased -100 V with respect to the satellite, effectively generating a 100 eV electron beam, with a current setting of 20 μA.

The data from these experiments are shown in spectrogram form in Figure 9. In this figure, data from the high energy electron detector (top) and low energy electron detector (bottom) are shown together. The satellite enters eclipse a few minutes into the period displayed here, and the locally generated electrons disappear. The satellite does not charge negatively during this eclipse, as evidenced by the lack of accelerated low energy ions in the ion detectors (not shown). This is typical for days when the plasma sheet electron fluxes have energies less than 10 keV [15]. When the filament is turned on, the satellite charges positively, up to near the bias voltage, as seen in the first sequence during eclipse. The subsequent experiments at higher bias voltages will be ignored, because of the relative lack of detector energy resolution at higher energies.

The satellite charged to near, but apparently less than 100 V. The change in the antenna potential is 90 V, indicating a satellite potential of 90-95 V with the gun on (This assumes a 1 or 2 V positive antenna potential with the gun off). The resulting electron distribution functions are shown in Figure 10. The distribution functions found here are similar to those seen in Figure 7. There is a peak, or plateau from 80-100 eV. The environment is much cooler on this day, and the ambient plasma density should be higher than that found on day 201. If the "emitter off" data are shifted in energy by about 80 eV, the distribution function overlaps the "emitter on" data. Hence, one interpretation of these data is that there are no changes in the plasma around the satellite due to the gun operation, simply an increase in satellite potential to about +80 V. There is an ambiguity to this interpretation, however, because the energy resolution of the detector ($\Delta E/E = 20\%$) is not high enough to distinguish between the possibility that the peak from 80-100 eV is simply accelerated ambient plasma, as opposed to heated (local) secondaries and low energy ambient plasma.

Journal of Electrostatics, 20 (1987) 43-57
Elsevier Science Publishers B.V., Amsterdam – Printed in The Netherlands

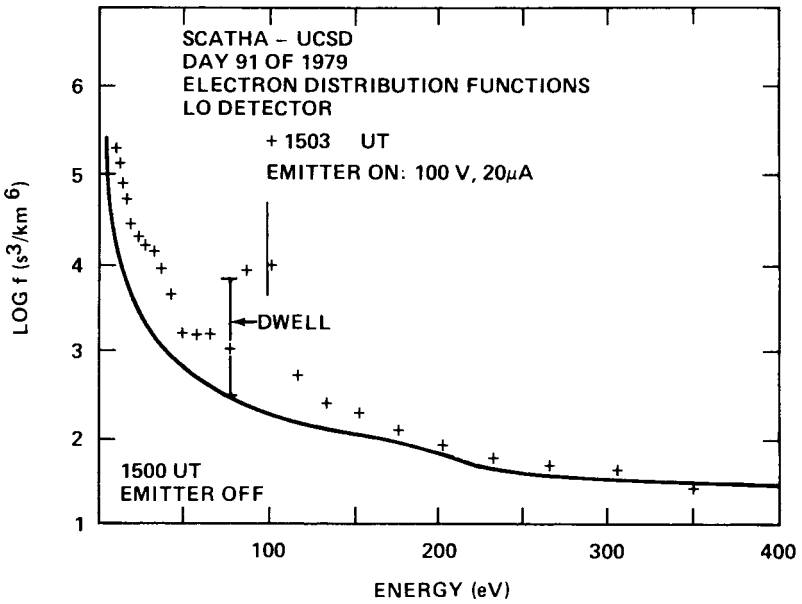

Figure 10. Electron distribution functions for 0 and 20 μA current levels, 100 V bias on the filament electron emitter.

III. NASCAP MODEL

The first step in analyzing these experiments requires modeling of the charging process, and the effects of charging on the particle data. The NASA Charging Analysis Program (NASCAP) is used for the charging analysis [16]. This code establishes a satellite model in an inner grid that is 16 x 16 x 33. This grid is embedded in up to 3 additional, coarser grids. The code solves for the currents to each surface cell, including the photocurrent and secondary electron currents, solves for the resulting potentials, and then solves Laplace's equation for the fields around the satellite. The code allows the user to specify the environment, and models the time evolution of the satellite potential. The model includes the capability to simulate an electron gun, and electrostatic analyzers. Space charge effects are not generally included in this code, which is appropriate for the geosynchronous environment for which the code was designed. First order corrections for space charge effects are included for the electron gun mode, in particular, the space charge limiting, or virtual anode effects, which occur when the satellite potential approaches the beam energy.

A simulation was run using an environment with density, n = 1 cm^{-3}, and temperature, T = 3 keV. [This latter, low value, was chosen to avoid substantial negative charging on the dielectrics. Such differential charging can also limit the beam current.] The model used here was developed by NASA, the Air Force, and S-Cubed (the NASCAP authors), to model charging on SCATHA. This development paid special attention to defining the surface material characteristics, which are the most critical aspect of charging at geosynchronous orbit. Initially, the satellite charges to about +3V in sunlight, with the gun off. The shadowed insulating surfaces on the 'bottom' of the satellite charge negatively by a few 10's of volts, particularly in the injection motor cavity, but this does not affect the rest of the satellite. (In a slightly hotter environment, this would eventually lead to negative mainframe potentials). The gun is then switched on, and the satellite potential promptly increases to +50V. The resulting potential distribution is shown in Figure 11a.

Journal of Electrostatics, 20 (1987) 43-57
Elsevier Science Publishers B.V., Amsterdam – Printed in The Netherlands

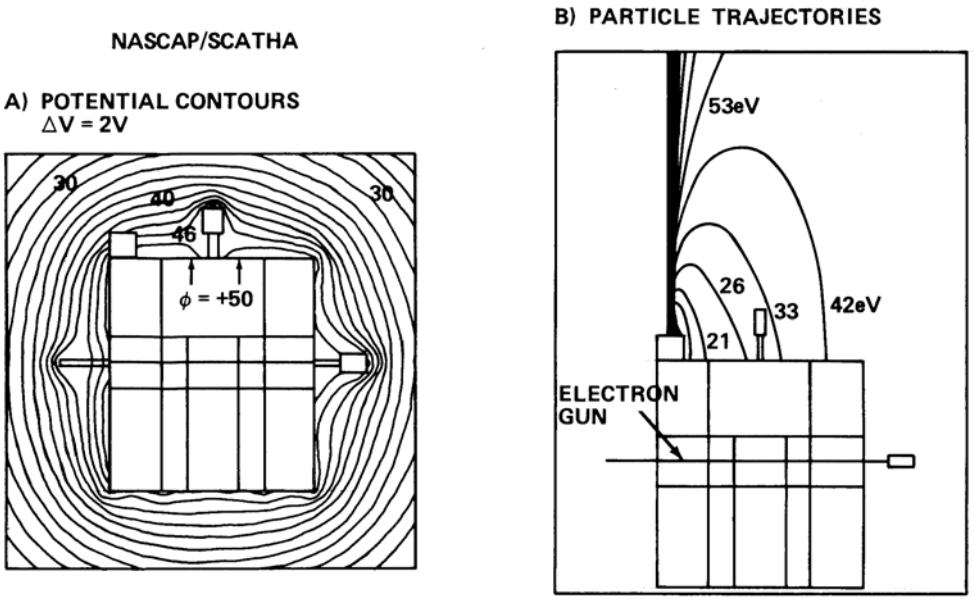

Figure 11. (a) NASCAP/SCATHA potential contours for a satellite charged to near beam energy. (b)NASCAP/SCATHA particle trajectories for electrons measured by UCSD detectors.

This figure shows potential contours in planes through the center of the satellite, and through the plane for the UCSD detectors. Aside from the negative charging in the injection motor cavity, the potential contours essentially show the monotonic decline expected with distance from the satellite. Figure llb shows the particle trajectories for the detector simulations. These are 'inside out' trajectories, i.e., test particles are emitted from the detector and tracked backwards until they reach infinity (the outer grid boundary) or return to the satellite. For detectors which are differential in angle, such as these, there is little mixing of trajectories. Below the satellite potential, there are only trajectories which lead back to the satellite, while above the satellite potential, trajectories lead to the distant plasma. Although these trajectories are distorted at low energies, for an isotropic environment, no change in the values of the distribution function result.

This modeling effort shows that the single-particle code successfully models the charging aspects of the electron gun operations. The detector simulation shows that the enhanced fluxes above the satellite potential are not a direct result of the increased satellite potential.

CONCLUSIONS

The electron gun operations on SCATHA conducted in sunlight resulted in charging of the satellite to potentials up to the beam energy, at beam currents which depended on the ambient plasma parameters. If the beam current is not high enough, the satellite charges to a potential below the beam energy. During the 10 μA experiment in the dusk bulge, no additional effects are inferred. However, during the 1 μA experiment in the lobe, an additional feature became apparent - the peak in the distribution function above the satellite potential. This feature continues to appear as the beam current increases, and the satellite potential rises to the beam energy. Complementary experiments in eclipse, in a low temperature plasma environment, produced ambiguous results. There was again a peak in the distribution function at energies above the inferred satellite potential, but these data are also consistent with measurements of cold ambient plasma accelerated into the detector by the increased satellite potential.

The peak in the daylight data is neither from the satellite main-frame, by conservation of energy, nor from the ambient plasma, by the shape of the distribution function. These electrons must be the result of interactions between the electron beam and the other electrons around the satellite. This latter population includes not only the ambient plasma, but the spacecraft generated photoelectron, which represent a higher

plasma density than the ambient (about 100 cm^{-3} vs. 1 cm^{-3}) in the region near the satellite. If the beam interacts with these other electrons, then scattering of the beam electrons could produce the plateau in the distribution function above the satellite potential. Also, the enhancement below the satellite potential can be explained as the result of heating the 'local' photoelectrons.

There is an alternative possibility for explaining the anomalous peak in the distribution function. This possibility is that photo-electrons or secondary electrons emitted from differentially charged surfaces could be reaching the detector. Although the peak is largely independent of pitch angle or detector look direction, if there was such a source, and these electrons were thermalized in some way, they could constitute the anomalous peak.

ACKNOWLEDGEMENTS

The author would like to thank the principal investigator for the electron gun experiment, Mr. Herb Cohen, for his aid in studying these data, and the principal investigator for the UCSD instrument, Dr. S. E. Deforest for making the study possible. Dr. T. L. Aggson was the PI for the electric field experiment, and provided that data for this study. Dr. C. E. Mcllwain and Dr. E. C. Whipple at the University of California at San Diego (UCSD) provided the means for analyzing the UCSD data. The operations staff at the Air Force Satellite Control Facility provided exceptional support of the real time experiments and data handling, which greatly improved the quality of our results. The NASCAPISCATHA model was graciously provided by Dr. M. J. Mandell, at S-Cubed. This work was supported by NASA Lewis Research Center under NAG3-620.

REFERENCES

1. Winckler, J. R., The application of artificial electron beams to magnetospheric research, Rev. of Geophysics and Space Physics, 18, 654-682, 1980.
2. Reasoner, D. L., J. L. Burch and T. Obayashi, Analysis of electron spectra produced by SEPAC electron beams on Spacelab-1 - Evidence for strong beam plasma interactions, EOS, 65, 1042, 1984.
3. Katz, I., G. A. Jongeward, D. E. Parks, D. L. Reasoner and C. K. Purvis, Energy broadening due to spacecharge oscillations in high current electron beams, Geophys. Res. Lett., 12, 64, 1986.
4. McPherson, D. A., D. P. Cauffman and W. R. Schober, Spacecraft charging at high altitudes: SCATHA satellite program, J. Spacecraft and Rockets, 12, 621-626, 1975.
5. Reasoner, D. L., W. Lennartsson and C. R. Chappell, Relationship between ATS6 spacecraft-charging occurrences and warm plasma encounters, Progress in Astronautics and Aeronautics, 47, Spacecraft Charging by Magnetospheric Plasmas, edited by A. Rosen, AIAA, pp. 89-101.
6. Olsen, R. C., Experiments in charge control of geosynchronous orbit - ATS5 and ATS6, J. Spacecraft and Rockets, 22, 254-264, 1985.
7. M. S. Gussenhoven, H. A. Cohen, D. A. Hardy, W. J. Burke and A. Chesley, Analysis of ambient and beam particle characteristics during the ejection of an electron beam from satellite near-geosynchronous orbit on March 30, 1979, in : N. J. Stevens and C. P. Pike (Eds.) , Spacecraft Charging Technology, 1980, NASA Conf. Publ. 2128, AFDGL-TR-81-0270, 1981, pp. 642-669.
8. H. A. Cohen, R. C. Adamo, T. Aggson, A. L. Chesley, D. M. Clark, S. A. Damron, D. E. Delorey, J. F. Fennell, M. S. Gussenhoven, F. A. Hanser, D. Hall, D. A. Hardy, W. B. Huber, I. Katz, H. C. Koons, S. T. Lai, B. Ledley, P. F. Mizera, E. G. Mullen, J. E. Nanevicz, R. C. Olsen, A. G. Rubin, G. W. Schnuelle, N. A. Saflekos, M. F. Tautz and E. C. Whipple, P78-2 Satellite and payload responses to electron beam operation on March 30, 1979, in: N. J. Stevens and C. P. Pike (Eds.), Spacecraft Charging Technology, 1980, NASA Conf. Publ. 2128, AFDGL-TR-81-0270, 1981, pp. 509-559.
9. Mauk, B. H., and C. E. Mcllwain, ATS6 UCSD Auroral particles experiment, IEEE Trans. Aerosp. El. Sys., AES-11, 1125-1130, 1975.
10. Aggson, T. L., P. G. Ledley, A. Egeland and I. Katz, Probe measurements of DC electric fields, from Spacecraft/plasma Interactions and their influence on field and particle measuremnts, proceedings of the 17th ESLAB Symposium, Noordwijk, The Netherlands, 13-16 September 1983, ESA, Special Publication 198, pp. 13-17, 1983.
11. Craven, P. D., R. C. Olsen, J. Fennell, D. Croley and T. L. Aggson, Potential modulation on the SCATHA spacecraft, Journal of Spacecraft and Rockets, in press, 1987.

12. Lai, S. T., H. A. Cohen and T. L. Aggson, The effect of photoelectrons on boom-satellite potential differences during electron beam ejection, EOS, 65, 1059, 1984.
13. Olsen, R. C., The hidden ion population of the magnetosphere, J. Geophys. Res., 87, 3481-3488, 1982.
14. Olsen, R. C., C. R. Chappell and J. L. Burch, Aperture plane potential control for thermal ion measurements, J. Geophys. Res., 91, 3117-3129, 1986.
15. Olsen, R. C., A threshold effect for spacecraft charging, J. Geophys. Res., 88, page 493, 1983.
16. M. J. Mandell, I. Katz, G. W. Schnuelle, P. G. Steen and J. C. Roche, The decrease in effective photocurrents due to saddle points in electrostatic potentials near differentially charged spacecraft, IEEE Transactions on Nuclear Science, vol 25, p 1313, 1978.